CONTOUR MAPS OF NORMALISED SCATTERED RADIATION DOSES AT DIFFERENT EYE HEIGHTS AND POSITIONS IN AN ANGIOGRAPHY ROOM BASED ON MULTIPLE LINEAR REGRESSION MODEL

Ahmad Radzi, H.[1*], Sohaimi, N.[1], Md Ralib, A.R.[2,3]

[1]Department of Diagnostic Imaging and Radiotherapy, Kulliyyah of Allied Health Sciences, International Islamic University Malaysia.
[2]Department of Radiology, Kulliyyah of Medicine, International Islamic University Malaysia.
[3]Department of Radiology, Sultan Ahmad Shah Medical Centre @IIUM.

Corresponding author: Halimatussa'diah Ahmad Radzi, International Islamic University Malaysia (IIUM), Jalan Sultan Ahmad Shah, Bandar Indera Mahkota, 25200 Kuantan, Pahang, MALAYSIA. Email: halimah@iium.edu.my.

Journal of Health Management, IHM

58

Vol. 20: No. 2/2023

ABSTRACT

Background: *The phantom study produced contour maps to educate angiography staff on the distributions of scattered radiation to their eyes.*

Methodology: *The scattered radiation came from an upper-body PBU-31 phantom (Kyoto Kagaku) exposed to percutaneous transhepatic biliary drainage technical factors. A total of 48 nanoDots™ (Landauer Inc.) were placed on the paper tubes, corresponding to six positions and eight heights (from 135 cm to 170 cm, with 5 cm increments) of the angiography staff's eyes from the scattered source. The studied projection and positions were posteroanterior (PA), 25° right anterior oblique (RAO), and 25° left anterior oblique (LAO). The measured doses (mGy) were normalised to the respective dose area product for each exposure (mGym^2). The normalised doses (mGy/mGym^2) were then transformed to their common logarithmic (log_{10}) form and analysed using a multiple linear regression model. After the analysis, the back transformation was performed, and the contour maps of the results were produced.*

Results: *Linear relationships were observed between log_{10} normalised scattered radiation doses with eye heights and positions for all projections [$F(6,137) = 56.96$, $p < .001$ (PA), $F(6,137) = 299.94$, $p < .001$ (25° RAO), $F(6,137) = 333.953$, $p < .001$ (25° LAO)]. An increase of 5 cm heights reduced normalised doses by 15.9%, 16.8%, and 6.7% in PA, 25° RAO, and 25° LAO, respectively. In PA projection, 155 cm and above eye heights received lower scattered radiation doses for all positions. Meanwhile, in 25° RAO, the flat panel detector (FD) shielded the position right next to the irradiated area. However, this position received higher scattered radiation doses in 25° LAO.*

Conclusion: *The contour maps differed for each projection, and the distribution of scattered radiation in an angiography room was affected by the shielding of the FD.*

Keywords: *angiography, radiation dosimetry, radiation protection, eye, occupational radiation exposure*
Manuscript classification: *Original research*

INTRODUCTION

Radiation exposure to the eyes of staff has become a topic of interest in recent years following the reduction of eye dose limit to the staff by the International Commission on Radiological Protection (ICRP) in 2011 (ICRP, 2012). Malaysia also followed the new dose limit of only 20 mSv per year (averaged over defined periods of five years, with no annual dose exceeding 50 mSv in any single year) instead of the previous limit (150 mSv per year) (Ministry of Health Malaysia, 2016). The tighter limit was because the eye lens is susceptible to radiation damage and may develop radiation-induced cataracts (Ainsbury et al., 2016). Therefore, it is important to study the factors that affect the amount of scattered radiation doses to the staff's eyes.

The position of the staff in the angiography room is an important factor to be studied, as radiologists who are closer to the patient receive higher doses to their eyes than those who are farther away (Alnaaimi et al., 2021; Bhar et al., 2021). Additionally, shorter staff receive higher doses due to their eye height (Gangl et al., 2022; Koenig et al., 2020; Principi et al., 2016). In this current study, scattered radiation distributions were measured at eight eye heights relevant to the Malaysian population and six positions near the examination table.

The study aimed to produce contour maps of normalised scattered radiation doses to nanoDots™ on the paper tubes that correspond to staff eyes at different heights and positions in an angiography room. The maps can be used for radiation protection training purposes. With the maps, the staff may recognise the safe distances in the angiography room and the risk of receiving higher eye doses based on their eye height. In addition, the study findings also identified which eye heights were not shielded by the flat panel detector (FD).

METHODOLOGY

A biplane C-arm angiographic system (Artis Q by Siemens Medical Solution Inc., Erlangen, Germany) was used in this study. However, only single-plane exposures from the floor-mounted C-arm were performed. The venue of the radiation exposure was Angiography Suites, Department of Radiology, SASMEC @IIUM. After each exposure, the dose area product (DAP) was recorded.

This study used an upper male body phantom (Kyoto Kagaku PBU-31) made of epoxy resin and polyurethane to simulate the patient's body and its x-ray attenuation properties. The phantom was exposed to percutaneous transhepatic biliary drainage (PTBD) technical factors in digital subtraction angiography (DSA) acquisition mode. Three radiographic projections were studied: i) posteroanterior (PA) projection; ii) 25° right anterior oblique (RAO) position; and iii) 25° left anterior oblique (LAO) position. For each projection, three radiation exposures were done to increase the accuracy of the radiation measurement.

The scattered radiation doses at different positions and heights at the side of the examination table were measured using 48 nanoDots™ of the Optical Stimulated Luminescence Dosimeter (OSLD) system by Landeuer, Inc. (Glenwood, IL, USA). Additional four nanoDots™ were placed outside the examination room as control nanoDots™. The stored radiation information in the nanoDots™ was read by the InLight®

MicroStar reader system, which was located at the Kulliyyah of Allied Health Sciences.

During scattered measurement, an adapted jungle gym method was used consisting of paper tubes and plastic joints developed by Dr Ikuo Kobayashi (Ito et al., 2019). Six 1.8 m paper tubes held the nanoDots™ at six positions beside the examination table. The side distance between the paper tubes was 50 cm, while the front or back distance was 30.48 cm (one foot). Eight slots were attached for each paper tube for the nanoDots™ to measure scattered radiation doses at 135 to 170 cm (with 5 cm increments) from the floor. Meanwhile, the distance between the second paper tube to the irradiation centre on the upper body phantom was 40 cm (**Figure 1**).

As for the radiation measurement calculation, the mean of three consecutive readings of nanoDots™ was calculated to increase the accuracy of readings (Ito et al., 2019; Kry et al., 2020). Then, the reading was deducted with the control nanoDots™'s reading to remove any noise due to the mechanical of the reader or the background radiation. In this study, the scattered radiation doses were then normalised to the DAP measurement as the tube voltage, current, and pulse width were controlled by the Automatic Dose Rate Control (ARDC) and were varied between exposures. The normalised doses enabled the data to be independent of exposure settings and can be used to compare doses of different settings (Stratakis et al., 2006).

The normalised scattered radiation doses were analysed using multiple linear regression (MLR) in IBM® SPSS® software version 25. The analysis models the relationship between the studied variables to predict the normalised scattered radiation doses with changing eye heights and positions. The dependent variable, the normalised scattered radiation doses in this analysis, was transformed to their common logarithmic (Laerd Statistics, 2015). The position variable was treated as categorical, and dummy variables were used during the analysis.

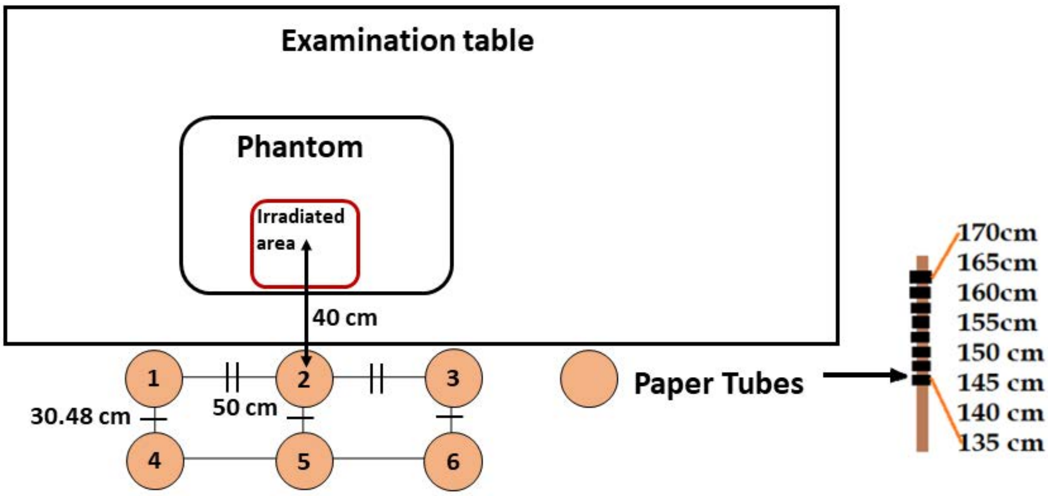

Figure 1: *The studied six positions at the side of the examination table and eight eye heights*

Back-transformation was performed when presenting the results, and the change in regression coefficient is interpreted as a change in ratio instead of unit change (Lee, 2020). Three scatter contour graphs were produced using Phyton version 3.10.7 with the integrated development environment (IDE) of Visual Studio Code (VS Code) version 1.74.0.

RESULTS

For all studied radiographic projections, linear relationships between studied variables were observed. The multiple linear regression (MLR) results for each projection were presented in the following subsections.

The Posteroanterior (PA) Projection

It was observed that there is a linear relationship between the log_{10} normalised scattered radiation doses with the eye heights and positions, $F(6,137) = 56.95$, $p < .001$. The model could explain 70.1% of the log_{10} normalised scattered radiation doses to the eyes based on the eye heights and positions. After back-transformation, an increment of one, five, and 10 cm of the staff eye height reduced 3.4%, 15.9%, and 29.2% of the normalised scattered radiation doses to the staff eye, respectively. During the MLR analysis, the position variable was treated as categorical data, and Position 2 was compared to other positions. It was found that the regression coefficient for Positions 3, 4 and 6 did not significantly differ from Position 2 (**Table 1**).

Table 1: *MLR results for scattered radiation doses in PA projection, 25° RAO and 25° LAO positions*

Dependent variables (y)	Independent variables (x)	Coefficient value (B) [95% Confidence Interval]	p-value
PA Projection			
Normalised scattered radiation doses (log_{10})	Constant	0.989 [0.731, 1.246]	< .001***
	Eye heights	-0.015 [-0.017, -0.013]	< .001***
	Position 1	0.069 [0.003, 0.135]	.040*
	Position 3	-0.012 [-0.078, 0.054]	.711
	Position 4	0.034 [-0.032, 0.100]	.310
	Position 5	0.0126 [0.061, 0.192]	< .001***
	Position 6	0.010 [-0.056, 0.076]	.770
25° RAO Position			
Normalised scattered radiation doses (log_{10})	Constant	-0.297 [-0.549, -0.045]	.021*
	Eye heights	-0.016 [-0.017, -0.014]	< .001***
	Position 1	1.066 [1.002, 1.131]	< .001***
	Position 3	0.866 [0.801, 0.930]	< .001***
	Position 4	0.965 [0.900, 1.029]	< .001***
	Position 5	0.911 [0.847, 0.976]	< .001***
	Position 6	0.897 [0.832, 0.961]	< .001***

cont.

cont. ***table 1***

Dependent variables (y)	Independent variables (x)	Coefficient value (B) [95% Confidence Interval]	p-value
25° LAO Position			
Normalised scattered radiation doses (log_{10})	Constant	0.027 [-0.068, 0.121]	.576
	Eye heights	-0.006 [-0.007, -0.005]	< .001***
	Position 1	-0.248 [-0.272, -0.224]	< .001***
	Position 3	-0.334 [-0.358, -0.310]	< .001***
	Position 4	-0.396 [-0.420, -0.372]	< .001***
	Position 5	-0.314 [-0.338, -0.289]	< .001***
	Position 6	-0.440 [-0.464, -0.416]	< .001***

Note: Significant levels: *p < .05; **p < .01; ***p < .001
B = unstandardised regression coefficient.

Following the back-transformation, the predicted normalised doses in their original form were graphed to create a scatter contour. The scatter contour depicts the distribution of normalised scattered radiation at different heights for those six positions for PA projection (**Figure 2**). The scatter contour shows that the eye heights of 155 cm and above received lower normalised scattered radiation at all positions. The eye heights of 135 cm received higher scattered radiation doses, especially for Position 5. The scatter contour shows that the normalised radiation distribution is not uniform across different positions and eye heights.

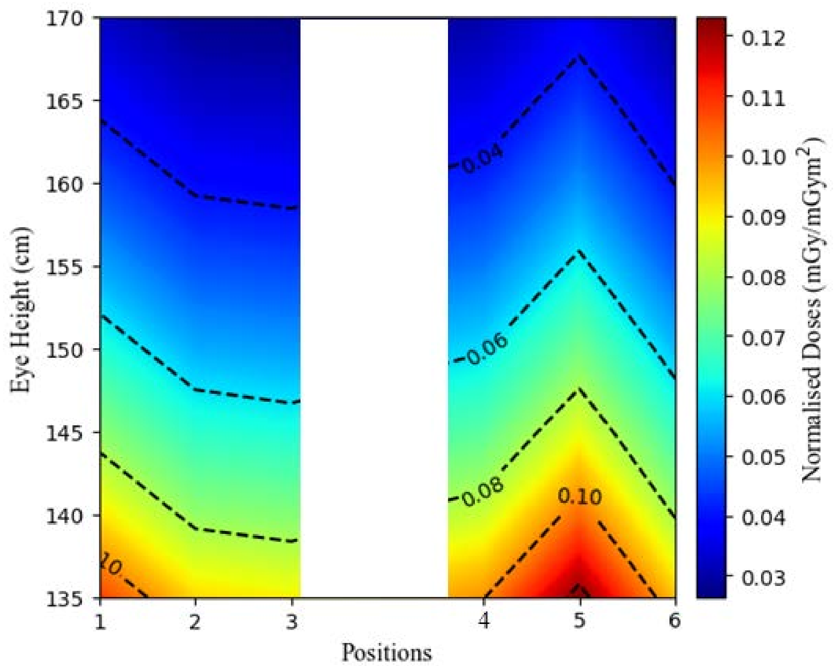

Figure 2: *The scatter contour at different eye heights and positions in PA projection*

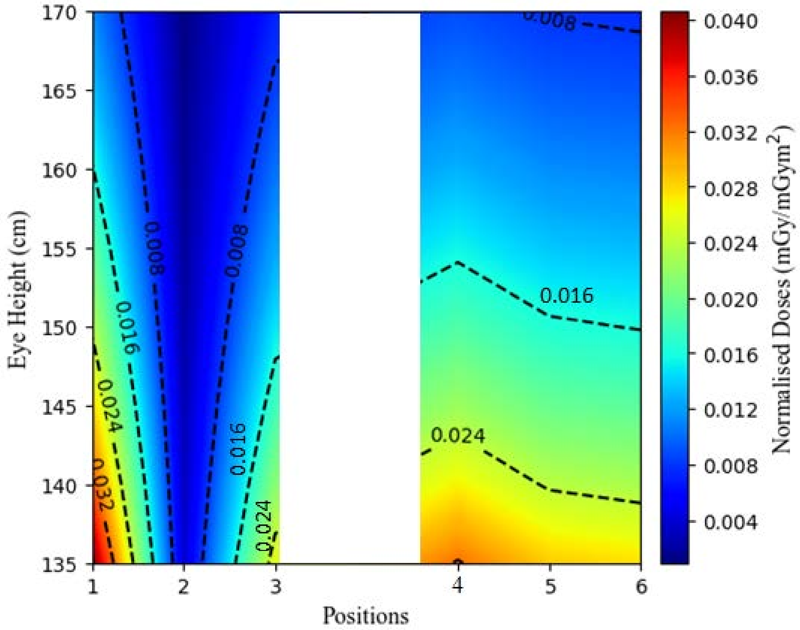

Figure 3: *The scatter contour at different eye heights and positions in 25° RAO position*

The 25° Right Anterior Oblique (RAO) Position

In this position, it was observed that there is a linear relationship between the $\log_{10}$ normalised scattered radiation doses to the eyes with eye heights and positions, $F(6,137) = 299.94$, $p < .001$. The model could explain 92.6% of the studied variables. It was found that a one, five, and 10-cm increase in eye height reduced 3.6%, 16.8%, and 30.8% of the normalised scattered radiation to the eyes, respectively. For this projection, all other position has significantly higher regression coefficient than Position 2 (**Table 1**).

The 25° RAO position's scatter contour was different from the finding in the PA projection's scatter contour. The normalised scattered radiations in Position 2 were lower than in the other positions for all eye heights. In addition, Position 5 also had lower scattered doses than Position 4 (**Figure 3**).

The 25° Left Anterior Oblique (LAO) Position

In this position, a linear relationship between the $\log_{10}$ of normalised scattered radiation and the eye height was also found, $F(6,137) = 333.953$, $p < .001$. The model could explain 93.3% of the studied variables. It was observed that Position 2 has a significantly higher regression coefficient than the other five positions (**Table 1**). An increase in one, five, and 10 cm increase in eye height reduces the normalised scattered radiation by 1.4%, 6.7%, and 12.9%, respectively.

It was observed that this position's scatter contour differed from the PA and 25° RAO projections. It was evident that Position 2 received higher scattered radiation doses than other positions, including for taller eye heights. However, the normalised scattered radiation doses were low at Positions 4, 5, and 6. However, Position 5 had higher scattered radiation than the adjacent two positions (**Figure 4**).

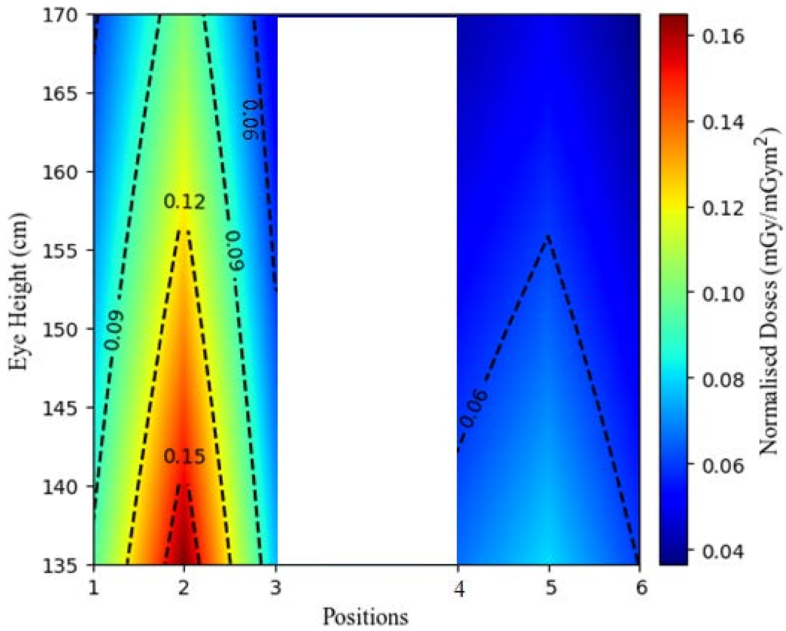

Figure 4: *The scatter contour at different eye heights and positions in 25° LAO position*

DISCUSSIONS

All doses presented in this study were the scattered radiation dose measures (mGy) using the nanoDot™ normalised to DAP. Thus, the normalised doses in this study can also be used as a comparison for other future studies regardless of technical factors. It is preferable to normalise the scattered radiation doses to DAP compared to the patient's doses, as this normalised dose enables adjustment based on the amount of radiation used (O'Connor et al., 2015).

The scatter contour maps produced in this study showed that the distribution of scattered radiation doses to the staff's eyes was non-uniform. This is supported by previous studies that found that the scattered radiation distribution in the angiography room was non-uniform and did not simply follow the inverse square law (Haqqani et al., 2013; Nowak et al., 2020).

The results from this current study also showed that the FD acted as a scattered radiation absorber, similar to the results by Principi et al., (2016) and Ferrari et al., (2022). However, the current study recognised the specific eye heights shielded by the FD. The FD caused a decrease in the distribution of normalised scattered radiation for eye heights above 155 cm at Position 2 (a common position for radiologists) in the PA projection and at all eye heights in Position 2 for the 25° RAO position. In PA projection, the scatter contour showed that those with eye heights of 155 cm and above received lower scattered radiation doses for all six positions. Meanwhile, in the 25° RAO position, this finding was also true except for Position 1. The eye height above 160 cm received lower doses for Position 1 of 25° RAO position. This current study found that the FD does not benefit eye heights lower than 155 cm. Therefore, the employer should give more attention to the staff with lower eye heights as they can be considered those with a higher risk receiving more scattered radiation to their eyes.

Besides that, it was found that the 25° LAO position resulted in more scattered radiation doses to the staff's eyes. This result agrees with other studies that found the LAO projection resulted in higher scattered radiation doses to the staff than other projections such as PA and RAO (Ferrari et al., 2022; Leyton et al., 2014). The possible explanation is that in this position, the FD no longer shields the staff from scattered radiation as it is rotated to the left of the phantom while the staff is on the right side (Ferrari et al., 2022). However, this is more applicable for positions near the phantom (Position 1, 2, and 3). The scattered radiation contour map showed low radiation doses at Positions 4, 5, and 6, located 30.48 cm at the back of Positions 1, 2, and 3.

This study had few limitations; one of them is that the subject was a phantom, and there are possible restrictions for generalising the result to the clinical settings. Nonetheless, the phantom study can provide the trend of change in outcome variables with changes in manipulated variables. Besides that, this study only involved the PTBD procedure with limited technical factor manipulation due to the limited time and funds available. Many other factors can affect the scattered radiation in the eyes of staff, and the scattered radiation field reaching the staff during the interventional procedure is rather complex (Ferrari et al., 2022). Therefore, the model created in this study may differ for the other types of procedures or other technical settings. In addition, the eye doses were measured in Hp (0.07) instead of Hp (3). However, this type of dosimeter is not widely available, and a dosimeter that measures Hp (10) and Hp (0.07) can also be used (IAEA, 2018).

CONCLUSION

In conclusion, contour maps of normalised scattered radiation doses to the staff eyes in an angiography room showed that distributions were non-uniform and different for all studied projections. The shielding provided by the FD affected the distribution. It was also found that the FD acts as a radiation absorber only for eye heights of more than 155 cm in the PA projection and 25° RAO position. Besides that, the information on the percentage decrease of scattered radiation doses with an increase in eye height (cm) may help the staff to realise how much scattered they are receiving compared to others due to their eye height.

A few recommendations for future works can be suggested based on the limitations discussed earlier. The model can be improved by adding more data with different technical factors. Besides that, it is also important to study more complex interventional procedures that involve higher patient radiation doses, such as neurological and cardiac studies. Another improvement for this research work is using dedicated eye dosimeters calibrated to Hp (3) instead of Hp (0.07), which provides a more accurate measurement of the eye lens doses.

ACKNOWLEDGEMENT

The authors thank the Kulliyyah of Allied Health Sciences (KAHS) and SASMEC @ IIUM for granting permission to conduct this study. The research was possible with the assistance given by members of the Department of Diagnostic Imaging and Radiotherapy (DDIR), KAHS and the Department of Radiology, SASMEC @IIUM.

The authors were also thankful to Dr. Ikuo Kobayashi for sharing his knowledge on the methods to measure scattered radiation dose using nanoDot™ OSLD and to Asst. Prof. Dr. Edre Mohammad Aidid for his statistical insights.

CONFLICT OF INTEREST

The authors declare that there is no conflict of interest.

REFERENCES

Ainsbury, E.A., Barnard, S., Bright, S., Dalke, C., Jarrin, M., Kunze, S., Tanner, R., Dynlacht, J.R., Quinlan, R.A., Graw, J., Kadhim, M., Hamada, N., 2016. Ionizing radiation induced cataracts: Recent biological and mechanistic developments and perspectives for future research. Mutation Research/Reviews in Mutation Research 770, 238–261.

Alnaaimi, M., Alduaij, M., Shenawy, F., Algaily, M., Mohammedzein, T., Shaaban, M., Rehani, M.M., 2021. Assessment of eye doses to staff involved in interventional cardiology procedures in Kuwait. Radiat Environ Biophys 60, 639–645.

Bhar, M., Mora, S., Kadri, O., Zein, S., Manai, K., Incerti, S., 2021. Monte Carlo study of patient and medical staff radiation exposures during interventional cardiology. Physica Medica 82, 200–210.

Ferrari, P., Ginjaume, M., Hupe, O., O'connor, U., Vanhavere, F., Bakhanova, E., Becker, F., Campani, L., Carinou, E., Clairand, I., Faj, D., Jansen, J., Jovanović, Z., Knežević, Ž., Krstić, D., Mariotti, F., Sans-Merce, M., Teles, P., Živković, M., 2022. What Is Worth Knowing in Interventional Practices about Medical Staff Radiation Exposure Monitoring: A Review of Recent Outcomes of EURADOS Working Group 12. Environments 9, 53.

Gangl, A., Deutschmann, H.A., Portugaller, R.H., Stücklschweiger, G., 2022. Influence of safety glasses, body height and magnification on the occupational eye lens dose during pelvic vascular interventions: a phantom study. Eur Radiol 32, 1688–1696.

Haqqani, O.P., Agarwal, P.K., Halin, N.M., Iafrati, M.D., 2013. Defining the radiation "scatter cloud" in the interventional suite. J Vasc Surg 58, 1339–1345.

IAEA, 2018. Radiation Protection and Safety in Medical Uses of Ionizing Radiation: Specific Safety Guide.

ICRP, 2012. ICRP Statement on Tissue Reactions / Early and Late Effects of Radiation in Normal Tissues and Organs - Threshold Doses for Tissue Reactions in a Radiation Protection Context, Annals of the ICRP. IRCP Publication 118. Ann.

Ito, H., Kobayashi, I., Watanabe, K., Ochi, S., Yanagawa, N., 2019. Evaluation of scattered radiation from fluoroscopy using small OSL dosimeters. Radiol Phys Technol 12, 393–400.

Koenig, A.M., Etzel, R., Greger, W., Viniol, S., Fiebich, M., Thomas, R.P., Mahnken, A.H., 2020. Protective Efficacy of Different Ocular Radiation Protection Devices: A Phantom Study. Cardiovasc Intervent Radiol 43, 127–134.

Kry, S.F., Alvarez, P., Cygler, J.E., DeWerd, L.A., Howell, R.M., Meeks, S., O'Daniel, J., Reft, C., Sawakuchi, G., Yukihara, E.G., Mihailidis, D., 2020. AAPM TG 191: Clinical use of luminescent dosimeters: TLDs and OSLDs. Med Phys 47, e19–e51.

Laerd Statistics, 2015. Multiple Regression Analysis using SPSS Statistics [WWW Document]. Statistical tutorials and software guides. URL https://statistics.laerd.com/spss-tutorials/multiple-regression-using-spss-statistics.php (accessed 8.14.22).

Lee, D.K., 2020. Data transformation: a focus on the interpretation. Korean J Anesthesiol 73, 503.

Leyton, F., Nogueira, M.S., Saad, J., dos Santos, J.A., Vano, E., Oliveira, M.A., Ubeda, C., 2014. Scatter radiation dose at the height of the operator's eye in interventional cardiology. Radiat Meas 71, 349–354.

Ministry of Health (MOH) Malaysia, 2016. Guideines On Occupational Radiation Protection in Medical Interventional Procedures.

Nowak, M., Carbonez, P., Krauss, M., Verdun, F.R., Damet, J., 2020. Characterisation and mapping of scattered radiation fields in interventional radiology theatres. Sci Rep 10, 1–9.

O'Connor, U., Walsh, C., Gallagher, A., Dowling, A., Guiney, M., Ryan, J.M., McEniff, N., O'Reilly, G., 2015. Occupational radiation dose to eyes from interventional radiology procedures in light of the new eye lens dose limit from the International Commission on Radiological Protection. Br J Radiol 88.

Principi, S., Farah, J., Ferrari, P., Carinou, E., Clairand, I., Ginjaume, M., 2016. The influence of operator position, height and body orientation on eye lens dose in interventional radiology and cardiology: Monte Carlo simulations versus realistic clinical measurements. Physica Medica 32, 1111–1117.

Stratakis, J., Damilakis, J., Hatzidakis, A., Perisinakis, K., Gourtsoyiannis, N., 2006. Radiation Dose and Risk from Fluoroscopically Guided Percutaneous Transhepatic Biliary Procedures. Journal of Vascular and Interventional Radiology 17, 77–84.